European Journal of Cell Biology 103 (2024) 151459

Contents lists available at ScienceDirect

European Journal of Cell Biology

journal homepage: www.elsevier.com/locate/ejcb

The expression level of VEGFR2 regulates mechanotransduction, tumor growth and metastasis of high grade serous ovarian cancer cells

Elisabetta Grillo [a,b,*], Cosetta Ravelli [a,b], Michela Corsini [a,b], Mattia Domenichini [a], Maria Scamozzi [a], Daniela Zizioli [a,b], Davide Capoferri [a], Roberto Bresciani [a,b,c], Chiara Romani [d,e], Stefania Mitola [a,b,*]

[a] Department of Molecular and Translational Medicine, University of Brescia, Via Branze 39, Brescia 25123, Italy
[b] The Mechanobiology research center, University of Brescia, Brescia, Italy
[c] Highly Specialized Laboratory, ASST Spedali Civili di Brescia, Piazzale Spedali Civili 1, Brescia 25123, Italy
[d] Angelo Nocivelli Institute of Molecular Medicine, ASST Spedali Civili of Brescia, Brescia, Italy
[e] Department of Medical and Surgical Specialties, Radiological Sciences and Public Health, University of Brescia, Brescia, Italy

ARTICLE INFO

Keywords:
VEGFR2
Ovarian cancer
HGSOC
Mechanotransduction
Cell motility
Metastasis

ABSTRACT

Recent data shows that alterations in the expression and/or activation of the vascular endothelial growth factor receptor 2 (VEGFR2) in high grade serous ovarian cancer (HGSOC) modulate tumor progression. However, controversial results have been obtained, showing that in some cases VEGFR2 inhibition can promote tumorigenesis and metastasis. Thus, it is urgent to better define the role of the VEGF/VEGFR2 system to understand/predict the effects of its inhibitors administered as anti-angiogenic in HGSOC. Here, we modulated the expression levels of VEGFR2 and analyzed the effects in two cellular models of HGSOC. VEGFR2 silencing (or its pharmacological inhibition) promote the growth and invasive potential of OVCAR3 cells *in vitro* and *in vivo*. Consistent with this, the low levels of VEGFR2 in OV7 cells are associated with more pronounced proliferative and motile phenotypes when compared to OVCAR3 cells, and VEGFR2 overexpression in OV7 cells inhibits cell growth. *In vitro* data confirmed that VEGFR2 silencing in OVCAR3 cells favors the acquisition of an invasive phenotype by loosening cell-ECM contacts, reducing the size and the signaling of focal adhesion contacts (FAs). This is translated into a reduced FAK activity at FAs, ECM-dependent alterations of mechanical forces through FAs and YAP nuclear translocation. Together, the data show that low expression, silencing or inhibition of VEGFR2 in HGSOC cells alter mechanotransduction and lead to the acquisition of a pro-proliferative/invasive phenotype which explains the need for a more cautious use of anti-VEGFR2 drugs in ovarian cancer.

1. Introduction

Ovarian cancer (OC) is a lethal gynecological cancer, with 313,959 new cases and 207,252 deaths worldwide in 2020 (WHO). High grade serous ovarian cancer (HGSOC) is the most frequent and aggressive histologic type. At diagnosis, most HGSOC patients present abdominal and/or distant metastases and the majority of them experience recurrence. The treatment of metastatic HGSOC remains a major clinical challenge as the therapeutic options often produce unsuccessful outcomes (Cannistra, 2004; Moffitt et al., 2019; Lisio et al., 2019). Among targeted therapies, interfering with the vascular endothelial growth factor (VEGF)/VEGF receptor 2 (VEGFR2) axis by modulating ligand bioavailability *via* anti-VEGF antibodies (i.e. bevacizumab) or by inhibiting the activity of the receptor *via* tyrosine kinase inhibitors (TKi) (e.g. pazopanib, cediranib, nintedanib and sorafenib) is a therapeutic approach approved or in clinical trial for HGSOC (Mei et al., 2023). Although these approaches were developed to block tumor angiogenesis, recent studies have highlighted that HGSOC cells express VEGFR2 and have an active VEGF/VEGFR2 axis, demonstrating that anti-angiogenic drugs also affect the tumor VEGF/VEGFR2 axis. However, anti-VEGFR2 drugs showed individual variability, limited efficacy and widespread resistance. In this context, it is remarkable that the VEGFR2 protein levels detected in tumor cells show a positive significant correlation with PFS in advanced-stage HGSOC (Guan et al., 2019). Consistent with this and similarly to other cancer types, VEGFR2 knockdown induces HGSOC cells to acquire an invasive phenotype

* Corresponding authors at: Department of Molecular and Translational Medicine, University of Brescia, Viale Europa 11, Brescia 25123, Italy.
E-mail addresses: elisabetta.grillo@unibs.it (E. Grillo), stefania.mitola@unibs.it (S. Mitola).

https://doi.org/10.1016/j.ejcb.2024.151459
Received 17 April 2024; Received in revised form 16 August 2024; Accepted 28 September 2024
Available online 1 October 2024

(Adham et al., 2010; Volz et al., 2020). These bodies of evidence question the prevailing perception of tumor VEGFR2 as an oncogene, suggesting instead that it may act as a tumor brake in HGSOC, and indicate that alterations in VEGFR2 could modulate the aggressiveness of HGSOC cells. This also implies that inhibition of tumor VEGF/VEGFR2 axis by anti-"angiogenic" drugs might be detrimental, possibly explaining the variable response/limited efficacy of these drugs in HGSOC. On these bases, there is an urgent need to clarify the promoting vs suppressive role of tumor VEGF/VEGFR2 axis in HGSOC in order to provide cancer patients with safe and efficacious targeted therapies.

In the attempt to fill this gap, we analyzed the role of VEGFR2 in two cellular models of HGSOC. VEGFR2 silencing in OVCAR3 cells enhances the tumorigenesis and metastasis *in vitro* and *in vivo*. To further investigate the association between the levels of VEGFR2 and cell growth and motility, we compared OVCAR3 with OV7 cells, which express significantly lower levels of VEGFR2. OV7 cells exhibit a more pronounced proliferative and motile behavior. Also, VEGFR2 overexpression in OV7 cells negatively regulated cell growth, confirming that VEGFR2 modulates HGSOC cells. Mechanistically, VEGFR2 levels modulate cell migration by controlling focal adhesion (FA) signaling, mechanical tension across FAs and mechanotransduction. Altogether, our data shed light on the role of the VEGF/VEGFR2 axis in limiting HGSOC progression and set the bases for a better evaluation of VEGFR2-targeted drugs in the treatment of OC patients.

2. Materials & methods

2.1. Cell cultures

Representative human HGSOC cell lines OVCAR3 and OV7 were purchased respectively from the European Collection of Authenticated Cell Cultures (ECACC) and Istituto Zooprofilattico Sperimentale della Lombardia e dell'Emilia Romagna (IZSLER, Brescia, Italy). OVCAR3 cells were maintained in RPMI medium supplemented with 20 % Fetal Bovine Serum (FBS, Gibco, ThermoFisher scientific, Carlsband, CA, USA), and 0.01 mg/mL bovine insulin (growt medium). OV7 cells were maintained in DMEM/HAMS F12 medium (Gibco) supplemented with 5 % FBS, 0.01 mg/mL bovine insulin, and 0.5 μg/mL hydrocortisone (growth medium). Cells were subcultured every three days and periodically checked to exclude mycoplasma contamination.

For VEGFR2 silencing, cells were infected with lentiviral particles harboring Mission® VEGFR2-targeting shRNAs. A single shRNA (TRCN0000001686) or a mix of four VEGFR2-targeting shRNAs were used to generate shVEGFR2-OVCAR3 or shVEGFR2mix-OVCAR3 cells, respectively. Cells transduced with non-targeting lentiviral particles (SCH202V) were named shCtrl-OVCAR3 and were used as controls in all experiments. Transduced cells were maintained in 1 μg/mL puromycin. For VEGFR2 overexpression cells were stably transfected with pBE_h-VEGFR2 plasmid using FuGENE (Promega, Milan, Italy). Transfected cell lines were maintained in 0.5 mg/mL geneticin.

2.2. Western blot analyses

Cells were lysed in lysis buffer [50 mM Tris-HCl buffer (pH 7.4), 150 mM NaCl, 1 % Triton X-100, 1 mM Na_3VO_4, and protease and phosphatase inhibitors (Sigma Aldrich, Milan, Italy). Next, lysates were separated by SDS-PAGE, transferred to PVDF membrane and probed with specific antibodies. Chemiluminescent signal was acquired by ChemiDoc™ Imaging System (Bio-Rad Laboratories, Providence, RI).

2.3. Cell proliferation

10×10^3 cells/cm^2 were cultured in DMEM 2 % FBS or growth medium in the absence or the presence of 50 ng/mL of recombinant VEGF-A for 48 h. Cell proliferation was measured by crystal violet colorimetric assay (OD 595 nm).

2.4. In vivo tumorigenesis

4×10^6 shVEGFR2-OVCAR3 or shCtrl-OVCAR3 cells were injected subcutaneously (s.c.) into the dorsolateral flank of NOD/SCID female mice (Envigo, Milan, Italy). Tumor volume was measured with calipers and calculated according to the formula $V=(Dxd^2)/2$, where D and d are the major and minor perpendicular tumor diameters, respectively. At the end of the experimental procedure, tumors were harvested, weighed, and processed for further analyses.

2.5. Immunofluorescence analyses

Cells seeded on collagen (Roche) (Coll)- or fibronectin (Sigma-Aldrich) (FN)-coated μ-slides or μ-dishes with an elastically supported surface with increasing rigidities (1.5, 15, 28 kPa; Ibidi) were incubated for 16 h and then fixed with 4 % PFA, permeabilized with 0.1 % Triton-X100 and immuno-decorated with the indicated antibodies. The actin cytoskeleton was decorated using fluorescently labeled phalloidin. Formalin-fixed paraffin-embedded tissue sections were immunodecorated using the indicated antibodies. Nuclei were counterstained with 4',6-diamidino-2-phenylindole (DAPI, Sigma-Aldrich). Samples were visualized by fluorescence microscopy, using a LSM880 confocal microscope (Carl Zeiss S.P.A.) and analyzed using ImageJ software.

2.6. Zebrafish embryo metastasis assay

The transgenic line *Tg(kdrl:mCherry)* was maintained at 28°C under a 14 h light/10 h dark cycle at pH 7.0–7.5 and conductivity 400–500 μs. OVCAR3 cells were stained with CellTracker Green CMFDA Dye (Molecular Probes, ThermoFisher scientific, Carlsband, CA, USA) and microinjected (~250 cells in 4 nL of PBS per embryo) into the duct of Cuvier of 48 hpf anesthetized (200 mg/L tricaine) *Tg(kdrl:mCherry)* zebrafish embryos using the electronic microinjector FemtoJet coupled with the InjectMan N12 manipulator (Eppendorf Italia, Milan, Italy). After injection, embryos were maintained at 33°C. After 4 h the accumulation of cells into the caudal vascular plexus (CVP) was evaluated by fluorescence microscopy.

2.7. FAT-FAK biosensor

FAT-FAK biosensor contains the ECFP/YPet FRET pair interspaced by a flexible linker and a FAK substrate sequence and the FAT domain for FA localization. By measuring the ECF/FRET emission ratio it enables to monitor FAK activity within FAs, as FAK can phosphorylate the Tyr residue within the substrate increasing the ECFP/FRET ratio (Wu et al., 2016). OVCAR3 cells transiently transfected with the FAT-FAK sensor and seeded onto Coll- or FN-coated μ-slides (Ibidi) for 16 h, were fixed and imaged using a LSM880 laser-scanning microscope (Carl Zeiss S.P.A, Oberkochen, Germany) equipped with a Plan-Apocrhromatic 63X/1,4 Oil DIC objective (Carl Zeiss). Images of ECFP and FRET channels were obtained exciting the biosensor at 458 nm and acquiring emissions at 515 ± 50 nm and 570 ± 50 nm, respectively. Images were then analyzed by Zen black 2.3 software to measure the ECFP/FRET ratio as a readout of FAK activity in FAs.

2.8. Mechanical tension

Cells were transiently transfected with the VinTS construct and seeded onto Coll- or FN-coated μ-slides (Ibidi) for 16 h. VinTS contains a TSMod elastic linker in between the mTFP1/Venus FRET couple, all cloned between the head and tail domains of vinculin protein. FRET was quantified by fluorescence lifetime imaging (FLIM) in live cells using an two-photon LSM880 laser-scanning microscope equipped with a Chameleon Vision II Ti:Sapphire pulsed laser (Coherent Inc, Santa Clara, CA, USA) and a FLIM system for time-correlated single-photon counting module (PicoQuant, Berlin, Germany). Of note, the FRET efficiency is

inversely proportional to the mechanical tension applied to vinculin (Grashoff et al., 2010). The fluorescence lifetime of mTFP1 was measured at 860 nm at an 80 MHz repetition rate. The decay curves were recorded and fitted using the SymphoTime 64 software version 2.2 (PicoQuant) to determine the donor lifetime in the absence or the presence of the acceptor (τDA/τD). FRET efficiencies (E) were calculated using the following equation: E=1−(τDA/τD)

2.9. Scratch assay

When indicated, culture plates were pre-coated with FN or Collagen. Cells were seeded at the density of 16×10^4 cells/cm^2 onto standard or CytoSoft® 6-well plates with increasing (0.5–16 kPa) rigidity (Advanced BioMatrix, Inc, Carlsbad, USA). After 16–24 h, confluent monolayers were scratched with a 200 μL tip and incubated in growth medium. Actin rich membrane protrusions, known as membrane ruffles, were counted after 4 h (Mitola et al., 2006a). After 24–48 h, monolayers were photographed, and the newly covered area was quantified by ImageJ software.

2.10. Scattering assay

Cells spheroids (800–1000 cells/each) were prepared by seeding cells in round-bottom 96-well plates in DMEM 0.4 % methylcellulose. Next, cell spheroids were harvested, resuspended in DMEM 2 %FBS and seeded onto standard plates in the presence of 50 ng/mL of recombinant VEGF-A or left untreated. After 48 h, spheroids were photographed and cell scattering was quantified by the formula (total area-spheroid area)/spheroid perimeter using ImageJ image analysis software (https://imagej.net/ij/download.html).

2.11. RT-qPCR

Total RNA was extracted using TRIzol Reagent (Invitrogen, TermoFisher) according to the manufacturer's instructions. Two μg of total RNA were retro-transcribed with MMLV reverse transcriptase (Invitrogen) using random hexaprimers. Then, cDNA was analyzed by qPCR using the primers listed in Table 1. Human *HPRT*, *ACTB*, *PP1A*, *GAPDH* and *SDHA* were analyzed as candidate endogenous controls. The most suitable endogenous control for normalization was selected based on the "gene stability score" [calculated using the QuantStudio Design & Analysis Software (ThermoFisher)]. Next, $2^{-\Delta\Delta Ct}$ was calculated. Data are expressed as relative expression ratios.

2.12. Boyden chamber cell migration assay

Cells suspended in serum free medium were seeded at 1×10^6 cells/mL in the upper compartment of a Boyden chamber containing gelatin-coated PVP-free polycarbonate filters (8μm pore size). Growth medium was placed in the lower compartment. After 4–16 h of incubation at 37°C, cells migrated to the lower side of the filter were stained with Diff-Quick reagent (Microptic) and quantified using ImageJ software.

2.13. Statistical analyses

Statistical analyses were performed using Prism 10.2.3 (GraphPad Software). Student's *t* test for unpaired data (2-tailed) was used to test the probability of significant differences between two groups of samples. Differences were considered significant when $p<0.05$ unless otherwise specified.

3. Results

3.1. VEGFR2 silencing sustains the tumorigenesis and metastatic dissemination of OVCAR3 cells

In order to investigate how VEGFR2 regulates the progression of HGSOC, we took advantage of representative human OVCAR3 HGSOC cells. A VEGFR2-targeting shRNA was used to knock down the receptor expression in OVCAR3 cells. Silencing was confirmed by comparing VEGFR2 expression in control (shCtrl) and silenced (shVEGFR2) cells by Western blot (WB) analyses (Fig. 1a). The reduction of VEGFR2 levels was accompanied by a decrease in the levels of pAkt and increased levels of pErk1/2 downstream mediators (Fig. 1a). Similar results were obtained when VEGFR2 expression was knocked down in OVCAR3 cells using a combination of 4 different shRNAs (shVEGFR2-mix) (Fig. S1a). These changes in intracellular signaling prompted us to explore how the low VEGFR2 expression affects the tumorigenic and metastatic capacity of HGSOC cells. As shown in Fig. 1b, VEGFR2 silencing accelerated OVCAR3 proliferation *in vitro*. Consistently, shVEGFR2-OVCAR3 cells showed a significantly increased tumorigenicity capacity *in vivo* compared to shCtrl-OVCAR3 cells (Fig. 1c-d). shVEGFR2-OVCAR3-derived tumors displayed increased vascularization compared to those derived from shCtrl-OVCAR3 cells, as demonstrated by the IF analysis of $CD31^+$ blood vessels (Fig. 1e-f).

Next, we investigated the metastatic capacity of shVEGFR2-OVCAR3 cells in an in *vivo* Zebrafish metastasis assay. Fluorescently labeled cells were injected into the duct of Cuvier of *Tg(kdrl:mCherry)* embryos at 48 hpf and their accumulation in the caudal vascular plexus (CVP) of embryos was monitored over time. As shown in Fig. 2, shVEGFR2-OVCAR3 disseminated more than control cells into the CVP. Again, this was confirmed also in shVEGFR2-mix-OVCAR3 cells (Fig S1b-c). Together these data corroborate the role of VEGFR2 in limiting the growth and dissemination of HGSOC cells.

3.2. VEGFR2 silencing alters focal adhesion signaling in OVCAR3 cells

The metastatic process involves a series of steps, including the

Table 1
List of primers used in the study.

Gene name	Forward	Reverse
KDR (VEGFR2)	GGAAATGACACTGGAGCCTA	TTTGAAATGGACCCGAGACA
TWIST	GTCCGCAGTCTTACGAGGAG	GCTTGAGGGTCTGAATCTTGCT
MMP2	GTATGGCTTCTGCCCTGAGA	CACACCACATCTTTCCGTCA
NCAD	CAACTTGCCAGAAAACTCCAGG	ATGAAACCGGGCTATCTGCTC
VIM	CGCCAGATGCGTGAAATG	ACCAGAGGGAGTGAATCCAGA
CD44	AACACCAAGCCCAGAGGAC	TCCAAATCTTCCACCAAACC
ALDH1A1	TCAGCAGGAGTGTTTACCAAAG	TCCCAGTTCTCTTCCATTTCC
OCLN	AGCAGCGGTGGTAACTTTGA	TTCCCTGATCCAGTCCTCCT
MMP10	GACAGAAGATGCATCAGGCAC	GGCGAGCTCTGTGAATGAGT
ACTB	CACACAGGGGAGGTGATAGC	GACCAAAAGCCTTCATACATCTCA
HPRT	CTTTCCTTGGTCAGGCAGTATAA	AGTCTGGCTTATATCCAACACTTC
GAPDH	GAAGGTCGGAGTCAACGGATT	TGACGGTGCCATGGAATTTG
SDHA	GGACAACTGGAGGTGGCATT	TTTTCTAGCTCGACCACGGC
PP1A	GAGGAAAACCGTGTACTATTAGC	GGGACCTTGTCTGCAAAC

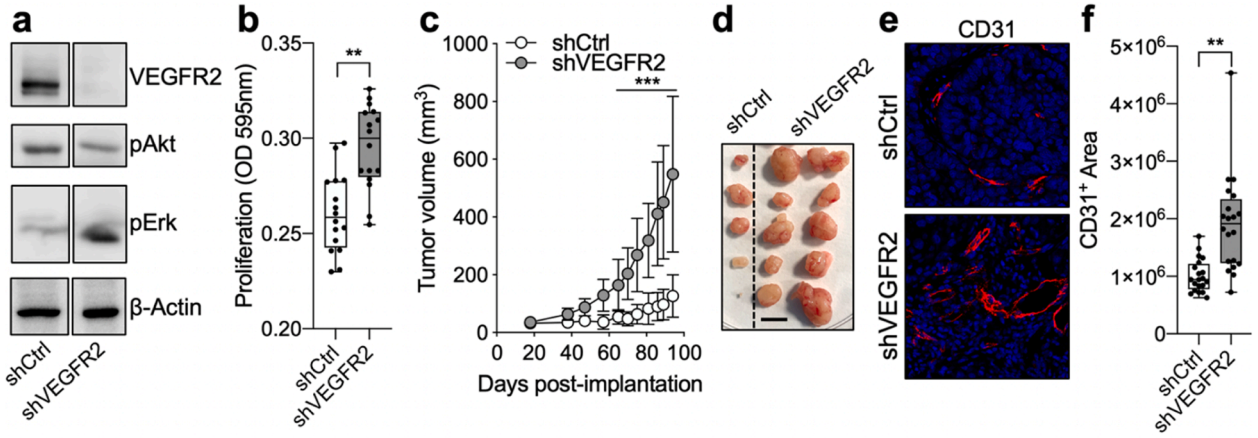

Fig. 1. VEGFR2 silencing promotes OVCAR3 cell proliferation, growth and metastasis. Western blot analysis of VEGFR2, phospho (p)-Akt and pErk1/2. β-actin was used as loading control. Non-adjacent lanes from the same blot are shown (see SIII) (**a**). *In vitro* cell proliferation in growth medium (**b**). *In vivo* growth of shVEGFR2-OVCAR3 and shCtrl-OVCAR3 cells implanted subcutaneously into the flank of NOD/SCID female mice (n=8–12) (**c**). Photographs of tumor xenografts are shown in (**d**) (scale bar 8.5 mm). Anti-CD31 analysis of FFPE sections of tumor xenografts (**e**). Quantification of $CD31^+$ area by image analysis (**f**). WB images are representative of 3 independent experiments that gave similar results. Individual values of each biological replicate obtained in 3 independent experiments are shown in Box and Whiskers graphs (points), where error bars represent min to max values. Data are shown as mean (SD) of biological replicates. Error bars, SD. **, $p<0.01$, ***, $p<0.005$ Student's *t* test.

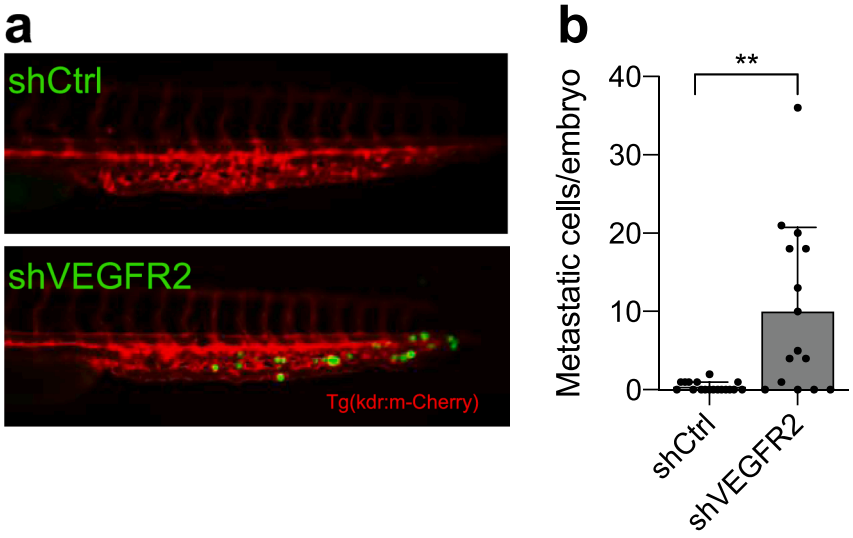

Fig. 2. VEGFR2 silencing promotes metastatic dissemination of OVCAR3 cells *in vivo*. Analysis of the metastatic spread of fluorescently labeled shVEGFR2-OVCAR3 and shCtrl-OVCAR3 cells into the caudal vascular plexus (CVP) of *Tg(kdrl:mCherry)* zebrafish embryos following injection in the duct of Cuvier. Representative images of CVP are shown (**a**). Represented values correspond to the mean (SD) of the number of cells accumulating at the CVP 4 h post-injection, n=15–25 injected embryos. Individual values of biological replicates are shown (points). Error bars, SD. Experiments were repeated three times (**b**). **, $p<0.01$, Student's *t* test.

coordinated regulation of cell adhesion, release of matrix degradation enzymes, cytoskeleton reorganization, cell migration and proliferation. Gaining insights into the bases of these processes is essential, as the disruption of any of these stages holds the potential to halt cancer dissemination. Each of these steps can be modeled *in vitro*. To delve into the role of VEGFR2 in regulating the metastatic spread of HGSOC, we analyzed the ability of shVEGFR2-OVCAR3 and shCtrl-OVCAR3 cells to adhere onto different ECMs and to organize their focal adhesions (FAs). Collagen (Coll) and fibronectin (FN) were selected, among others, given their role in regulating VEGFR2 activation (Soldi et al., 1999; Mitola et al., 2006b) and their dysregulation in OC (Sherman-Baust et al., 2003; Cheon et al., 2014; Natarajan et al., 2019; Kenny et al., 2014; Bao et al., 2021). The number of cells adherent to Coll and FN after 24 h was similar for shCtrl-OVCAR3 and shVEGFR2-OVCAR3 cells (90–95 % of total seeded cells). Despite this, we detected significant changes in the organization and signaling of FAs. As shown in Fig. 3a-c, the silencing of VEGFR2 did not affect the number of FAs *per se*. Interestingly, it significantly reduced by 28–40 % the area of p-Paxillin$^+$ FAs in the basal portion of cells adherent to Coll and FN respectively when compared to shCtrl-OVCAR3 cells. Consistent results were obtained when shVEGFR2-mix-OVCAR3 cells were compared to shCtrl-OVCAR3 cells (Fig. S1d-f). To further characterize FA signaling we measured the kinase activity of FAK within FAs by transfecting OVCAR3 cells with the fluorescence resonance energy transfer (FRET)-based FAT-FAK biosensor (Wu et al., 2016). By analyzing cells adherent to ECMs we detected a significant reduction in FAK activity when shCtrl-OVCAR3 cells were seeded onto FN compared to the same cells seeded on Coll. In this context, VEGFR2 silencing further reduces FAK activity when

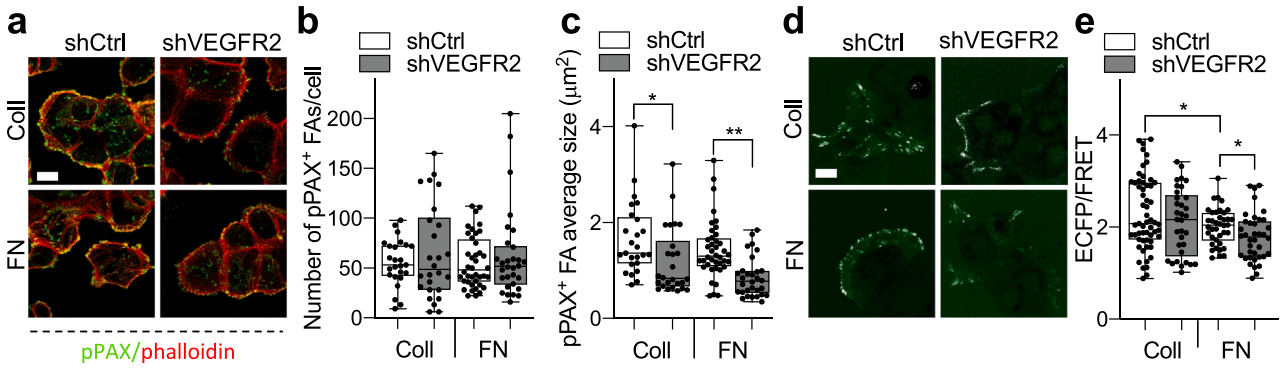

Fig. 3. VEGFR2 silencing alters focal adhesion signaling in OVCAR3 cells. IF analysis of pPAX in cells adherent to collagen- (Coll) or fibronectin (FN)-coated μ-slides. F-Actin was decorated with phalloidin. The number/cell and average dimension (area) of pPAX^{+} FAs were analyzed and quantified by image software analyses. Scale bar 20 μm (**a-c**). Analysis of FAK activity in the FAs of cells transfected with FAT-FAK FRET-based sensor and adherent onto Coll- or FN-coated μ-slides. Scale bar 30 μm (**d-e**). ECFP/FRET ratio images are shown in **d**. ECFP/FRET ratio was calculated using Zen Software and is shown in (**e**). Individual values of each biological replicate derived from 3 independent experiments are shown in Box and Whiskers graphs (points), where error bars represent min to max values. *, p = 0.027 (**c**), 0.048 and 0.037 (**e**); **, p<0.01, Student's *t* Test.

cells are adherent to FN, while it does not significantly modify the activity of FAK in FAs in cells seeded onto Coll (Fig. 3d,e). Overall, this data point to a role of VEGFR2 in the modulation of FA-associated signaling in HGSOC cells.

3.3. VEGFR2 silencing increases the mechanotransduction in OVCAR3 cells

FAs are nanoscale complexes of structural and signaling molecules (including FAK, PAX, vinculin etc.) that link the ECM to the cytoskeleton, and function as principal sites of mechanotransduction, a molecular process that translates mechanical cues applied to cells into intracellular biochemical signals. To explore the role that VEGFR2 plays in mechanotransduction, we visualized the mechanical tension across shVEGFR2-OVCAR3 and shCtrl-OVCAR3 cells. To this, we exploited the FLIM/FRET-based Vinculin tension sensor (VinTS) (Grashoff et al., 2010). This sensor enables the analysis of the mechanical tension applied on vinculin. Control and silenced OVCAR3 cells were transfected with the VinTS construct and plated onto Coll or FN. Imaging analyses showed that the adhesion of shCtrl-OVCAR3 on FN increases FRET efficiency in the FAs with respect to Coll-seeded cells, demonstrating the generation of lower tension forces. In this context, VEGFR2 silencing significantly decreased FRET efficiency in cells plated on FN, indicating an increased tension across vinculin. Instead, in cells adherent to Coll, VEGFR2 knock-down leads to increased VinTS sensor FRET efficiency compared to shCtrl-OVCAR3 cells, supporting a looser cell-substrate adhesion (Fig. 4a-b). Next, we evaluated whether the changes in the tension across vinculin upon VEGFR2 silencing modify the localization of the mechanosensor YAP. As demonstrated by immunofluorescence analyses, YAP was mainly localized within the nucleus in shCtrl-OVCAR3 cells seeded on Coll and VEGFR2 silencing did not impact its localization. On the other hand, the adhesion onto FN maintained YAP in the cell cytoplasm and in close contact with p-PAX^{+} FAs in shCtrl-OVCAR3 cells. In this context, VEGFR2 silencing promoted YAP translocation into the nucleus (Fig. 4c). This confirms that the VEGF/-VEGFR2 axis and ECM control the mechanotransduction in HGSOC cells. Thus, the ECM remodeling in OC deserves further attention as it may impact the response to targeted therapies.

3.4. VEGFR2 silencing promotes the acquisition of a pro-migratory phenotype in OVCAR3 cells

To continue the characterization of the role of VEGFR2 in controlling the metastatic dissemination of HGSOC cells, we evaluated the effects of VEGFR2 silencing on cell migration. As anticipated, VEGFR2 knock-down significantly promoted the migratory capacity of OVCAR3 cells. This was highlighted by the higher number of membrane ruffles (Fig. 5a) and by the increase of the newly covered area (Fig. 5b) exhibited by

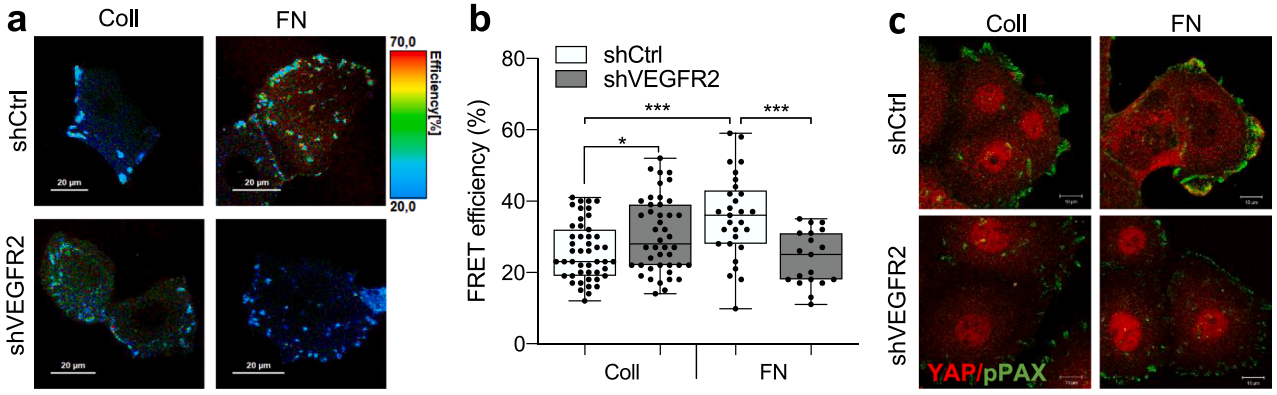

Fig. 4. VEGFR2 silencing alters mechanotransduction in OVCAR3 cells. FRET images of VinTS sensor in cells adherent to Coll or FN. FRET was quantified by fluorescence lifetime imaging (FLIM). Color-coded FRET efficiency is shown in representative pictures. Scale bar 20 μm. Individual values of each biological replicate derived from 3 independent experiments are shown in Box and Whiskers graphs (points), where error bars represent min to max values. *, p = 0.021; ***, p<0.005, Student's *t* Test. (**a-b**). IF analysis of YAP and pPAX in shCtrl-OVCAR3 and shVEGFR2-OVCAR3 cells adherent to Coll or FN. Scale bar 10 μm (**c**).

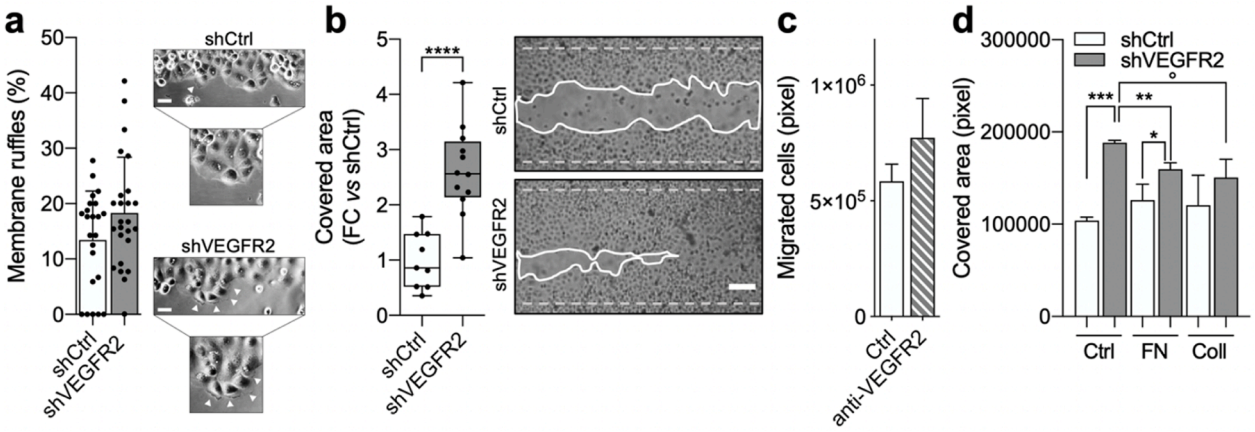

Fig. 5. VEGFR2 silencing sustains OVCAR3 cell motility. Analysis of migration of shCtrl-OVCAR3 and shVEGFR2-OVCAR3 cells in a scratch assay (**a-b**). Membrane ruffles were counted in n=10 fields 1 h after the scratch. Data are shown as the mean (SD) of three independent experiments. Error bars, SD. Representative pictures and magnification are shown. Scale bar 50 μm. Arrowheads, membrane ruffles (**a**). Calculated newly covered area and representative images of wounded monolayers after 48 h are shown in **b** (scale bar 300 μm). Individual values of each biological replicate derived from 3 independent experiments are shown in Box and Whiskers graphs (points), where error bars represent min to max values. ****, $p<0.001$, Student's *t* test. Migration of OVCAR3 cells in a Boyden chamber in the absence or the presence of neutralizing anti-VEGFR2 antibody (**c**). Scratch assay of shCtrl-OVCAR3 and shVEGFR2-OVCAR3 cells seeded onto uncoated (Ctrl) or FN/Coll-coated (1 μg/mL) plates (**d**). Data are shown as the mean (SD) of three independent measurements. Error bars, SD. *, $p=0.036$, **, $p<0.01$, ***, $p<0.005$ Student's *t* test.

shVEGFR2-OVCAR3 cells when compared to shCtrl-OVCAR3 cells in a scratch assay *in vitro*. Similar results were obtained with shVEGFR2-mix-OVCAR3 cells (Fig. S1g-h) and when OVCAR3 cells were treated with an anti-VEGFR2 neutralizing antibody in a Boyden chamber migration assay (Fig. 5c). Finally, we assessed the contribution of ECM on the collective cell migration. To this, a scratch assay was performed on shCtrl-OVCAR3 and shVEGFR2-OVCAR3 cells seeded onto FN or Coll-coated culture plates. Regardless the type of underlying ECM, the motility of shCtrl cells was not affected in a significant manner, while the migration of shVEGFR2-OVCAR3 cells was slowed down when cells were adherent to FN or Coll compared to uncoated plates. However, shVEGFR2-OVCAR3 cells maintained a higher motility than control cells (Fig. 5d). On the other hand, ECM coating did not affect the proliferation of both shVEGFR2- and shCtrl-OVCAR3 cells (Fig. S2). Noticeably, VEGFR2-silenced cells displayed increased expression of *VIM*, *CD44*, *MMP2* and *MMP10* markers and decreased levels of *ALDH1A1* and *OCLN* (Fig. S3). All the features exhibited by OVCAR3 cells upon VEGFR2 knock-down (i.e. high motility, expression of *VIM*, *CD44* markers) resemble the recently characterized fast-progressing and aggressive claudin-low subtype of HGSOC (Romani et al., 2021).

In addition to the type of substrate (i.e. ECM), the adhesive/motile phenotype of ovarian cancer cells is also influenced by the stiffness of the substrate (Fan et al., 2021). Thus, we analyzed the effect of VEGFR2 silencing on cell motility in a scratch assay as a function of substrate stiffness (0.5–28 kPa). The Paxillin phosphorylation was followed to evaluate the FA activity. As expected, phospho-paxillin increased with substrate stiffness in shCtrl-OVCAR3 cells. Instead, silenced cells displayed very low pPAX staining (Fig. 6a) compared to control cells and pPAX levels did not change with varying substrate stiffness (Fig. 6a). This suggests that cells with low VEGFR2 expression could be less responsive to changes in substrate rigidity. We next investigated cell motility in a scratch assay performed on a 0.5 or 16 kPa stiff substrate. Under both conditions, shVEGFR2-OVCAR3 cells repaired the scratch significantly faster than control cells. The increase in substrate stiffness significantly increased the repair of the scratch by shCtrl-OVCAR3 cells, while exerting a milder effect (not significant) on shVEGFR2-OVCAR3 cells (Fig. 6b). This confirmed that VEGFR2 silencing hampered the responsiveness of OVCAR3 cells to changes in extracellular stiffness.

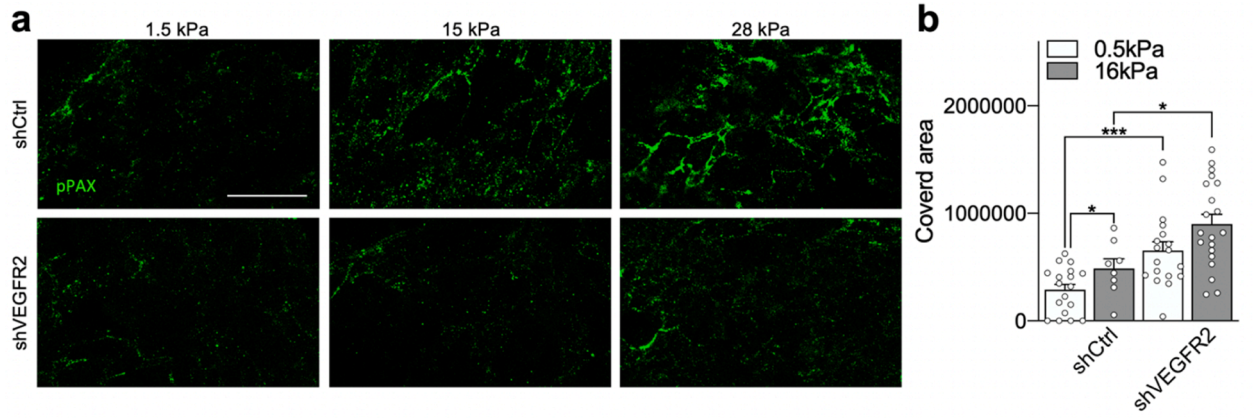

Fig. 6. VEGFR2 silencing modifies the response of OVCAR3 cells to changes in substrate stiffness. pPax staining of shVEGFR2-OVCAR3 or shCtrl-OVCAR3 cell monolayers grown onto FN-coated μ-dishes with an elastically supported surface with increasing rigidities (1.5–28kPa) (**a**). Scratch assay of shVEGFR2-OVCAR3 or shCtrl-OVCAR3 cell monolayers adherent to Coll-coated CytoSoft® 6-well plates with increasing (0.5–16 kPa) rigidity. Data are shown as mean of two independent experiments. Error bars, SEM. *, <0.05; ***, $p<0.005$, Student's *t* test.

3.5. Low levels of VEGFR2 are associated with a proliferative and motile phenotype in HGSOC cells

To verify how the levels of VEGFR2 modulate the behavior of HGSOC cells we selected an additional representative and well-characterized HGSOC cell line, namely OV7 cells. Of note, these cells express significantly lower levels of VEGFR2 compared to OVCAR3 cells (Fig. 7a). As shown in Fig. 6b, overexpression of VEGFR2 in OV7 cells elicits opposite outcomes as compared to VEGFR2 knockdown in OVCAR3 cells, as it significantly decreases by more than 50 % the cell clonogenic capacity *in vitro*. Also, by comparing OVCAR3 with OV7 cells we demonstrated that "VEGFR2-low" OV7 cells displayed a more pronounced proliferative and migratory capacity (Fig. 7c-d), paralleled by a higher expression of invasion-related genes, including the EMT markers *N-CAD* and *TWIST*, and *MMP2* compared to "VEGFR2-high" OVCAR3 cells (Fig. 7f). Of note, VEGF-A stimulation did not affect the *in vitro* proliferation of OVCAR3 and OV7 cells (Fig. 6f-g). On the contrary, VEGF-A stimulated both OVCAR3 and OV7 cell scattering (Fig. 7h-i). Together, this data confirmed that VEGFR2 expression levels regulated cell proliferation and motility in two HGSOC cell models and suggested that VEGFR2 expression levels and VEGFR2 activation may act independently to regulate the phenotype of HGSOC cells.

In conclusion, our data collectively demonstrate that VEGFR2 limits the growth, motility and invasiveness of HGSOC cells *in vitro* and *in vivo,* by modulating cell-ECM mechanotransduction, and suggest that VEGFR2 inhibition should be carefully considered in HGSOC patients to avoid unwanted and detrimental effects.

4. Discussion

The VEGF/VEGFR2 pathway is commonly considered to exert pro-tumoral effects and this has justified the development and the use of targeted drugs in cancer treatment. However, recent preclinical and clinical data have questioned this concept, showing instead that inhibition of the VEGF/VEGFR2 pathway, under certain circumstances, may induce tumors to acquire a pro-metastatic phenotype. This evidence has opened the urgent question of how this axis is regulated in the different cancers, to guide therapeutic choices and avoid unwanted and detrimental effects. Here we demonstrated that low levels of VEGFR2 expression and/or its inhibition in two cellular models of HGSOC sustain tumor proliferation, motility and invasion. Our data confirm previous findings showing that VEGFR2 silencing in OVCAR3 cells leads to increased tumor cell proliferation (Adham et al., 2010) and reveal for the first time the role of VEGFR2 in limiting the motility and metastatic potential of HGSOC cells. These findings add a piece of knowledge about the role of VEGFR2 in HGSOC. In addition, the silencing or the inhibition of VEGFR2 promotes the growth and vascularization of tumors that may ultimately support unwanted pro-metastatic features of HGSOC cells. Although further studies are necessary to corroborate these new concepts, a greater attention should be paid to the administration of anti-VEGFR2 drugs to OC patients in light of the results shown in this study.

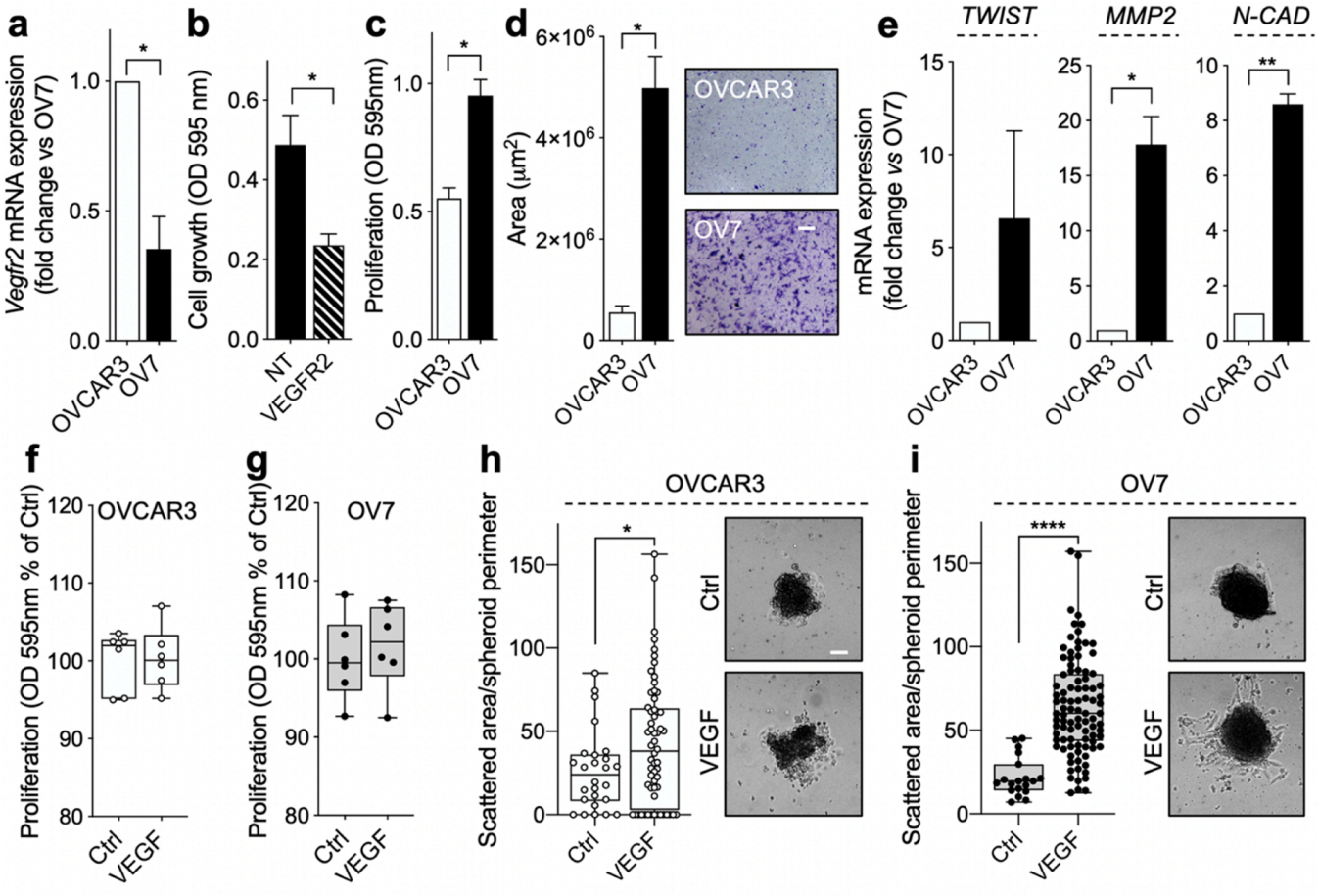

Fig. 7. Comparison of OVCAR3 and OV7 cell lines. mRNA levels of VEGFR2 measured by qPCR (**a**). Analysis of the *in vitro* clonogenic capacity of OV7 and OV7-VEGFR2 cells (**b**). *In vitro* cell proliferation (**c**) and migration (**d**) of OVCAR3 and OV7 cells in growth medium. mRNA levels of motility-related genes measured by qPCR. *ACTB* was used as endogenous control for normalization (**e**). *In vitro* cell proliferation (**f-g**) or scattering (**h-i**) of OVCAR3 or OV7 cells left untreated (Ctrl) or stimulated with 50 ng/mL of recombinant VEGF-A for 48 h in DMEM 2 % FBS. Representative pictures of scattered cells are shown. Scale bars, 100 μm. Data are shown as the mean (SD) of three independent measurements. Error bars, SD. *, $p<0.05$, **, $p<0.01$, ****, $p<0.001$, Student's *t* test.

To investigate the impact of low-VEGFR2 expression in HGSOC we compared OVCAR3 and OV7 cells, which endogenously express high and low levels of the receptor, respectively. These experiments confirmed that low levels of VEGFR2 are associated with increased proliferation and motility. Of note, OV7 cells have been recently characterized as a model of claudin-low (CL)-HGSOC tumors, typically characterized by decreased expression of claudins and other epithelial markers, increased expression of mesenchymal and stemness markers, altered metabolism, increased metastatic potential and reduced response to carboplatin (Romani et al., 2021). Data suggest that VEGFR2 downregulation may be part of the gene program activated in fast migrating/fast-progressing CL-HGSOC. We also addressed the complementary question whether VEGFR2 activation inhibits HGSOC motility and proliferation. Our results suggest that VEGFR2 levels and VEGFR2 activation may act independently in the regulation of HGSOC cell biology. However, these aspects could have a profound impact on the therapeutic choices for HGSOC patients and deserve further investigation.

HGSOC cells mostly exfoliate from the primary lesions, survive anoikis, attach to the mesothelial lining of the peritoneum and invade this epithelial layer to metastasize abdominal organs. This process, known as transcoelomic dissemination, remains the major cause of death in OC (Naora and Montell, 2005). Cell-ECM interactions and mechanical forces regulate multiple steps of OC cell motility and metastasis. Rigid/fibrotic ECM with altered collagen fibril density/topology is found in primary and metastatic OC (McKenzie et al., 2018). OC cells express ECM-stiffening enzymes and use mechanical forces to attach and invade the mesothelial layer (Iwanicki et al., 2011). In turn, mesothelial cells actively promote early OC metastasis by increased production of fibronectin (Kenny et al., 2014). The impact of VEGFR2 inhibition on the motile and invasive capacity led us to hypothesize that VEGFR2 could regulate cell-ECM interactions and mechanotransduction in HGSOC cells.

Components of the cellular mechanosensing system include integrins, FAs, actin cytoskeleton and associated molecular motors that together convert mechanical cues into ion fluxes and/or intracellular signaling. Mechanotransduction occurring at FAs dictates how cells attach, spread and move onto ECM. In the long term, mechanical signals through FAs regulate gene expression and alter cell behavior (Nelson and Bissell, 2006). In this context, FAs are the pivotal complexes (more than 100 different proteins can be recruited in FAs) that take contacts with ECM and coordinate the assembly of intracellular adhesion complexes and transmit mechanical signals. In turn, FAs are very well-known foci of signal transduction of RTKs, including VEGFR2. VEGFR2 is found within FAs in endothelial cells, it activates the kinase activity of FAK inside or outside FAs and modulates the cytoskeleton reorganization. Consistent with this paradigm, data shows that VEGFR2 levels modulate the organization and signaling of FAs. In particular, VEGFR2 silencing in OVCAR3 cells leads to a reduction of the area of $pPAX^{+}$ FAs and of FAK activity within FAs. Based on this data, it is reasonable to speculate that the lack of VEGFR2 may hamper protein recruitment at FAs, resulting in less FAK activity. This is consistent with a looser cell-substrate adhesion and may explain the increased motility and metastatic capacity of OVCAR3 cells detected both *in vitro* and *in vivo*. Our data are consistent with previous findings showing that small FAs are associated with a highly motile phenotype in metastatic cancer cells (Sharifi et al., 2016) and that paxillin downregulation promotes endothelial cell migration (German et al., 2014).

FAs are master regulators of mechanotransduction. FA maturation leads to the activation of the Hippo-YAP/TAZ signaling pathways which eventually results in YAP nuclear translocation. Consistent with this, VEGFR2 silencing affects FA reorganization and signaling, the mechanical tension across vinculin and the localization of YAP in OVCAR3 cells. Of note, the different mechanical effects of VEGFR2 silencing on different ECMs could reflect the role of fibronectin and collagen in the regulation of receptor activation (Soldi et al., 1999; Mitola et al., 2006b). In this context, it is important to remember that both collagen and fibronectin are dysregulated in OC where they sustain cancer progression and metastatic spread (Sherman-Baust et al., 2003; Cheon et al., 2014; Natarajan et al., 2019; Kenny et al., 2014; Bao et al., 2021) and VEGFR2 expression may collaborate in the modulation of cancer progression. However, Coll or FN coating did not significantly alter the motility of control OVCAR3 cells while decreasing the motility of VEGFR2-knocked-down OVCAR3 cells. Future studies will investigate how different ECMs and VEGFR2 levels could co-act to control HGSOC metastasis.

In addition to the type of ECM, substrate stiffness influences the motility of ovarian cancer cells (Fan et al., 2021). In our experimental conditions, VEGFR2 silencing reduces the responsiveness of OVCAR3 cells to changes in substrate stiffness, while increasing the sensitivity to changes in ECM composition (see above). These aspects deserve further investigation to understand whether VEGFR2 levels influence in a ECM-dependent (composition and/or stiffness) manner HGSOC dissemination. Of note, when cells were seeded onto substrates with a stiffness in the range of kPa (compared to glass/plastic substrates that have a stiffness in the order of GPa), paxillin was not recruited in the elongated anisotropic FAs, while it forms small cluster at cell-cell junctions (Fig. 6a) as previously reported for other FA proteins (Kleinschmidt and Schlaepfer, 2017). Localization of FA proteins out of FAs is not surprising. For example, structured illumination microscopy images and intensity profile analysis demonstrated that paxillin overlapped with cadherin (Bai et al., 2023).This may be due to, at least in part, a substantial lack of FAs in ovarian cancer cells adherent to substrates with a stiffness below 25 kPa (McKenzie et al., 2018). Also, it suggests that under biomimetic conditions, pPAX in OVCAR3 cells may have a role in cell-cell junction dynamics and collective migration. Further investigation is necessary to clarify how VEGFR2 silencing affects the response to substrate stiffness.

Only scattered evidence has shown that RTKs, including EGFR and VEGFR2, regulate mechanosensors (calpain 2, YAP/TAZ) (Wang et al., 2017; Schwartz et al., 2018). Our findings suggest that VEGFR2 levels control the mechanosensitivity of OC cells, being the first report of this role of VEGFR2 in cancer cells. These results open the way to the identification of novel druggable vulnerabilities that target mechanical cues in OC.

In our study we employed 2D cell models to characterize the role of VEGFR2 in HGSOC motility and mechanotransduction. More sophisticated 3D models could be used to further assess how VEGFR2 regulates cell-ECM and cell-cell interactions during the steps of HGSOC progression. In this context, invadopodia, key structures that contribute to the ability of cancer cells to invade and metastasize, could be analyzed and the unknown role of VEGFR2 in the regulation of these structures in HGSOC cells could be better characterized. These models could also help to understand how ECM-dependent force generation is linked to VEGFR2 levels. In particular they will help to clarify how VEGFR2 silencing increases force generation on FN, while decreasing it on Coll promoting in both cases cell motility.

Of note, VEGFR2 silencing in OVCAR3 cells using a single or a mix of 4 shRNAs exerted similar effects, confirming that VEGFR2 levels control mechanotransduction, motility, growth and metastasis of OVCAR3 cells. Further confirmation of the role of VEGFR2 in the OVCAR3 model derives from the similar effects of its pharmacological inhibition. Moreover, the comparison of VEGFR2-expressing OVCAR3 cell with OV7 cells, which express significantly lower levels of VEGFR2, showed that low VEGFR2 is associated with pronounced growth and motility. Finally, VEGFR2 overexpression in OV7 cells exerts opposite effects (i.e. reduction of proliferation) as compared to VEGFR2 silencing in OVCAR3 cells, corroborating the importance of VEGFR2 levels in controlling HGSOC cell behavior.

In conclusion, this study highlights the unprecedented role of VEGFR2 in altering mechanotransduction through FAAs and in limiting the proliferation and motility of HGSOC cells. Our report adds to a

growing body of work that shows that VEGFR2 expression in cancer cells, in certain contexts, can block tumor progression rather than promoting it. Together with other studies, our results suggest that greater attention should be paid to the use of anti-VEGFR2 drugs for OC patients.

CRediT authorship contribution statement

Davide Capoferri: Investigation. **Roberto Bresciani:** Investigation. **Chiara Romani:** Investigation, Conceptualization. **Stefania Mitola:** Writing – review & editing, Supervision, Project administration, Funding acquisition, Conceptualization. **Maria Scamozzi:** Investigation. **Daniela Zizioli:** Investigation. **Michela Corsini:** Investigation. **Mattia Domenichini:** Formal analysis, Investigation. **Elisabetta Grillo:** Writing – review & editing, Investigation, Formal analysis, Conceptualization. **Cosetta Ravelli:** Writing – original draft, Methodology, Investigation, Formal analysis.

Ethics approval

In vivo experiments, approved by Italian "Ministero della Salute" [authorizations 266/2016-PR and DM 92/2009-A (19.05.2009)- C. L.2.4.05], were performed in accordance with national and European guidelines and regulations for laboratory animal use in research.

Declaration of Competing Interest

The authors declare that they have no known competing financial interests or personal relationships that could have appeared to influence the work reported in this paper.

Data availability

Data will be made available on request.

Acknowledgements

The authors are grateful to Prof. Marco Presta (University of Brescia, Italy) for helpful discussion. The authors performed experiments at the Zebrafish Facility and at the Imaging Platform of the Department of Translational and Molecular Medicine of the University of Brescia.

This work was supported by grants from Associazione Italiana Ricerca sul Cancro to S.M. (AIRC grant IG17276), from University of Brescia (Fondi ex 60 %) to R.B., D.Z. and S.M., from "PNRR M4C2-Investimento 1.4-CN00000041 finanziato dall'Unione Europea-NextGenerationEU" to S.M and M.C. M.C was supported by Associazione Italiana per la Ricerca sul Cancro (ID 26917-2021). M.S. was supported by MIUR to Consorzio Interuniversitario per le Biotecnologie (CIB). E.G. and D.C. were supported by Fondazione Umberto Veronesi Fellowships. Funding bodies did not have any role in designing the study, collecting, analyzing, and interpreting data or in writing the manuscript.

Authors' contributions

E.G. and S.M. designed the study. E.G., C.R., M.C., M.D.,M.S., D.Z., R. B., D.C., C.R. and S.M. conceived and performed experiments; E.G., C.R. and S.M interpreted the results and wrote the manuscript. All authors read and approved the final manuscript.

Appendix A. Supporting information

Supplementary data associated with this article can be found in the online version at doi:10.1016/j.ejcb.2024.151459.

References

Adham, S.A., Sher, I., Coomber, B.L., 2010. Molecular blockade of VEGFR2 in human epithelial ovarian carcinoma cells. Lab Invest. 90 (5), 709–723. https://doi.org/10.1038/labinvest.2010.52.

Bai, M., Zhang, Z., Chen, H., Liu, X., Xie, J., 2023. Paxillin tunes the relationship between cell-matrix and cell-cell adhesions to regulate stiffness-dependent dentinogenesis. Regen. Biomater. 10, rbac100. https://doi.org/10.1093/rb/rbac100.

Bao, H., Huo, Q., Yuan, Q., Xu, C., 2021. Fibronectin 1: a potential biomarker for ovarian cancer. Dis. Markers 2021, 5561651. https://doi.org/10.1155/2021/5561651.

Cannistra, S.A., 2004. Cancer of the ovary. N. Engl. J. Med. 351 (24), 2519–2529. https://doi.org/10.1056/NEJMra041842.

Cheon, D.J., Tong, Y., Sim, M.S., Dering, J., Berel, D., Cui, X., et al., 2014. A collagen-remodeling gene signature regulated by TGF-beta signaling is associated with metastasis and poor survival in serous ovarian cancer. Clin. Cancer Res. 20 (3), 711–723. https://doi.org/10.1158/1078-0432.CCR-13-1256.

Fan, Y., Sun, Q., Li, X., Feng, J., Ao, Z., Li, X., et al., 2021. Substrate stiffness modulates the growth, phenotype, and chemoresistance of ovarian cancer cells. Front. Cell Dev. Biol. 9, 718834. https://doi.org/10.3389/fcell.2021.718834.

German, A.E., Mammoto, T., Jiang, E., Ingber, D.E., Mammoto, A., 2014. Paxillin controls endothelial cell migration and tumor angiogenesis by altering neuropilin 2 expression. J. Cell Sci. 127 (Pt 8), 1672–1683. https://doi.org/10.1242/jcs.132316.

Grashoff, C., Hoffman, B.D., Brenner, M.D., Zhou, R., Parsons, M., Yang, M.T., et al., 2010. Measuring mechanical tension across vinculin reveals regulation of focal adhesion dynamics. Nature 466 (7303), 263–266. https://doi.org/10.1038/nature09198.

Guan, J., Darb-Esfahani, S., Richter, R., Taube, E.T., Ruscito, I., Mahner, S., et al., 2019. Vascular endothelial growth factor receptor 2 (VEGFR2) correlates with long-term survival in patients with advanced high-grade serous ovarian cancer (HGSOC): a study from the Tumor Bank Ovarian Cancer (TOC) Consortium. J. Cancer Res. Clin. Oncol. 145 (4), 1063–1073. https://doi.org/10.1007/s00432-019-02877-4.

Iwanicki, M.P., Davidowitz, R.A., Ng, M.R., Besser, A., Muranen, T., Merritt, M., et al., 2011. Ovarian cancer spheroids use myosin-generated force to clear the mesothelium. Cancer Discov. 1 (2), 144–157. https://doi.org/10.1158/2159-8274.CD-11-0010.

Kenny, H.A., Chiang, C.Y., White, E.A., Schryver, E.M., Habis, M., Romero, I.L., et al., 2014. Mesothelial cells promote early ovarian cancer metastasis through fibronectin secretion. J. Clin. Invest. 124 (10), 4614–4628. https://doi.org/10.1172/JCI74778.

Kleinschmidt, E.G., Schlaepfer, D.D., 2017. Focal adhesion kinase signaling in unexpected places. Curr. Opin. Cell Biol. 45, 24–30. https://doi.org/10.1016/j.ceb.2017.01.003.

Lisio, M.A., Fu, L., Goyeneche, A., Gao, Z.H., Telleria, C., 2019. High-grade serous ovarian cancer: basic sciences, clinical and therapeutic standpoints. Int. J. Mol. Sci. 20 (4). https://doi.org/10.3390/ijms20040952.

McKenzie, A.J., Hicks, S.R., Svec, K.V., Naughton, H., Edmunds, Z.L., Howe, A.K., 2018. The mechanical microenvironment regulates ovarian cancer cell morphology, migration, and spheroid disaggregation. Sci. Rep. 8 (1), 7228. https://doi.org/10.1038/s41598-018-25589-0.

Mei, C., Gong, W., Wang, X., Lv, Y., Zhang, Y., Wu, S., et al., 2023. Anti-angiogenic therapy in ovarian cancer: current understandings and prospects of precision medicine. Front. Pharm. 14, 1147717. https://doi.org/10.3389/fphar.2023.1147717.

Mitola, S., Belleri, M., Urbinati, C., Coltrini, D., Sparatore, B., Pedrazzi, M., et al., 2006a. Cutting edge: extracellular high mobility group box-1 protein is a proangiogenic cytokine. J. Immunol. 176 (1), 12–15. https://doi.org/10.4049/jimmunol.176.1.12.

Mitola, S., Brenchio, B., Piccinini, M., Tertoolen, L., Zammataro, L., Breier, G., et al., 2006b. Type I collagen limits VEGFR-2 signaling by a SHP2 protein-tyrosine phosphatase-dependent mechanism 1. Circ. Res. 98 (1), 45–54. https://doi.org/10.1161/01.RES.0000199355.32422.7b.

Moffitt, L., Karimnia, N., Stephens, A., Bilandzic, M., 2019. Therapeutic targeting of collective invasion in ovarian cancer. Int. J. Mol. Sci. 20 (6). https://doi.org/10.3390/ijms20061466.

Naora, H., Montell, D.J., 2005. Ovarian cancer metastasis: integrating insights from disparate model organisms. Nat. Rev. Cancer 5 (5), 355–366. https://doi.org/10.1038/nrc1611.

Natarajan, S., Foreman, K.M., Soriano, M.I., Rossen, N.S., Shehade, H., Fregoso, D.R., et al., 2019. Collagen remodeling in the hypoxic tumor-mesothelial niche promotes ovarian cancer metastasis. Cancer Res. 79 (9), 2271–2284. https://doi.org/10.1158/0008-5472.CAN-18-2616.

Nelson, C.M., Bissell, M.J., 2006. Of extracellular matrix, scaffolds, and signaling: tissue architecture regulates development, homeostasis, and cancer. Annu. Rev. Cell Dev. Biol. 22, 287–309. https://doi.org/10.1146/annurev.cellbio.22.010305.104315.

Romani, C., Capoferri, D., Grillo, E., Silvestri, M., Corsini, M., Zanotti, L., et al., 2021. The Claudin-low subtype of high-grade serous ovarian carcinoma exhibits stem cell features. Cancers (Basel) 13 (4). https://doi.org/10.3390/cancers13040906.

Schwartz, A.D., Hall, C.L., Barney, L.E., Babbitt, C.C., Peyton, S.R., 2018. Integrin alpha6 and EGFR signaling converge at mechanosensitive calpain 2. Biomaterials 178, 73–82. https://doi.org/10.1016/j.biomaterials.2018.05.056.

Sharifi, M.N., Mowers, E.E., Drake, L.E., Collier, C., Chen, H., Zamora, M., et al., 2016. Autophagy promotes focal adhesion disassembly and cell motility of metastatic tumor cells through the direct interaction of paxillin with LC3. Cell Rep. 15 (8), 1660–1672. https://doi.org/10.1016/j.celrep.2016.04.065.

Sherman-Baust, C.A., Weeraratna, A.T., Rangel, L.B., Pizer, E.S., Cho, K.R., Schwartz, D. R., et al., 2003. Remodeling of the extracellular matrix through overexpression of collagen VI contributes to cisplatin resistance in ovarian cancer cells. Cancer Cell 3 (4), 377–386. https://doi.org/10.1016/s1535-6108(03)00058-8.

Soldi, R., Mitola, S., Strasly, M., Defilippi, P., Tarone, G., Bussolino, F., 1999. Role of alphavbeta3 integrin in the activation of vascular endothelial growth factor receptor-2. EMBO J. 18 (4), 882–892. https://doi.org/10.1093/emboj/18.4.882.

Volz, C., Breid, S., Selenz, C., Zaplatina, A., Golfmann, K., Meder, L., et al., 2020. Inhibition of tumor VEGFR2 induces serine 897 EphA2-dependent tumor cell invasion and metastasis in NSCLC. Cell Rep. 31 (4), 107568. https://doi.org/10.1016/j.celrep.2020.107568.

Wang, X., Freire Valls, A., Schermann, G., Shen, Y., Moya, I.M., Castro, L., et al., 2017. YAP/TAZ Orchestrate VEGF signaling during developmental angiogenesis. Dev. Cell 42 (5), 462–478. https://doi.org/10.1016/j.devcel.2017.08.002 e7.

Wu, Y., Zhang, K., Seong, J., Fan, J., Chien, S., Wang, Y., et al., 2016. In-situ coupling between kinase activities and protein dynamics within single focal adhesions. Sci. Rep. 6, 29377. https://doi.org/10.1038/srep29377.